ELSEVIER

Quaternary Science Reviews 23 (2004) 1151–1171

QG QSR

Stratigraphy and geochronology of pitfall accumulations in caves and fissures, Bermuda

Paul J. Hearty[a,*], Storrs L. Olson[b], Darrell S. Kaufman[c,d], R. Lawrence Edwards[e], Hai Cheng[e]

[a] *School of Earth Sciences, James Cook University, Townsville, Qld., 4811, Australia*
[b] *National Museum of Natural History, Smithsonian Institution, Washington, DC 20560, USA*
[c] *Department of Geology, Northern Arizona University, Flagstaff, AZ 86011-4099, USA*
[d] *Department of Environmental Sciences, Northern Arizona University, Flagstaff, AZ 86011-4099, USA*
[e] *Department of Geology and Geophysics, University of Minnesota, Minneapolis, MN 55455, USA*

Accepted 30 September 2003

Abstract

Deep fractures (“fissures”) and avens (“skylights”) in limestone cave roofs create natural traps for sediments and biota. Fissures fill quickly with surface sediment and organisms soon after opening. Debris cones are formed as materials fall, wash, or drift on air through openings in cave skylights. Such deposits in Admiral’s and Grand Canyon Cave, Bermuda contain distinct beds and are composed of mixtures of sediment and charcoal, together with fossils of land snails, crabs, birds, reptiles, and bats. The “pitfall” accumulations were periodically sealed over by calcite flowstone. A stratigraphic record of surface activity and fauna through both glacial and interglacial periods has been preserved. The succession also provides an ideal setting in which to compare several geochronological methods. Calibrated ^{14}C ages on charcoal and shells provide dated horizons at 1600, 12,800, and about 35,000 ^{14}C yr BP. Thermal ionization mass spectrometric (TIMS) ages on several flowstone layers constrain the entire sequence in the Admiral’s Cave sequence between 126,300 ± 900 yr (Termination II) and historical times. A continuous relative-age record generated by amino acid epimerization (AAE) geochronology (D-alloisoleucine/L-isoleucine or aIle/Ile) on the pulmonate land gastropod *Poecilozonites* verifies the biostratigraphy, reveals a minimal degree of mixing between stratigraphic units, and establishes an independent temporal link between the subterranean and subaerial deposits of Bermuda. This convergence between stratigraphy and geochronology yields a precisely dated succession from the oceanic island of Bermuda, and thus presents a unique opportunity to assess the rates and processes of evolutionary and climate change during that interval.

1. Introduction

Bermuda holds an important place in the study of Quaternary geology (see Curran and White, 1995) and evolutionary theory (Gould, 1969; Eldredge and Gould, 1972). The island has one of the world’s most complete documented records of Quaternary sedimentation as related to sea-level highstands. A supposed radiation of land snails of the genus *Poeciliozonites* provided Gould (1969) with material for several essays on evolution, as well as one of the prime examples used in the original promulgation of the theory of “punctuated equilibria” (Eldredge and Gould, 1972). These snails came from surface samples in eolianite and weak soils of interglacial age, and from caves and fissure fills that were undated but incorrectly assumed to be older than most or all of the surface deposits. Eolianite deposits are abundant on the island, and preservation potential of fossil snails in them is high. Gould’s sampling was heavily biased (85%) toward the eolianite portion of the fossil record, which comprises only a fraction of the temporal record of Bermuda. Indeed, in the model advocated by Eldredge and Gould (1972), the “punctuation” of equilibria may inadvertently reflect large gaps in sampling, a lack of age control, and an incomplete and inaccurate understanding of the stratigraphic succession. Glacial-age surface sediments, which constitute the balance of the record, are generally thin, heavily leached, and rarely contain any fossils.

*Corresponding author. Tel.: +61-0747815283.
E-mail address: paul.hearty@jcu.edu.au (P.J. Hearty).

0277-3791/$ - see front matter © 2003 Elsevier Ltd. All rights reserved.
doi:10.1016/j.quascirev.2003.09.008

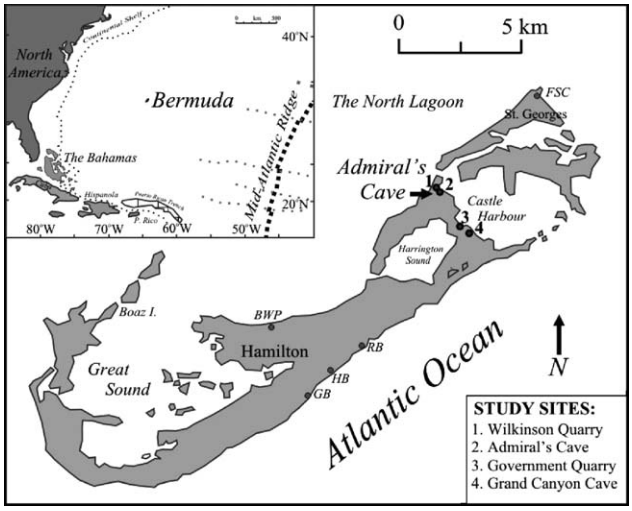

Fig. 1. Location of Bermuda in the North Atlantic Ocean showing the main study sites (legend). Other abbreviations: BWP, Blackwatch Pass; FSC, Fort St. Catherine; RB, type locality of Rocky Bay Formation; HB, Hungry Bay; GB, type locality of new Grape Bay Member.

Due to the accumulation and preservation of pitfall deposits in caves and fissures, an extensive part of the "missing" record has been retrieved and reconstructed. Both glacial and interglacial deposits are preserved in Admiral's Cave (ADC), Grand Canyon Cave (GCC), and numerous fissure deposits mostly centered on the western margin of Castle Harbour in Bermuda. This study presents a new and detailed stratigraphic, biostratigraphic, aminostratigraphic, and geochronologic record that spans the period from the marine isotope stage (MIS) 6/5e transition (Termination II) to historical times on Bermuda.

Bermuda is situated about 1000 km E of Cape Hatteras, North Carolina (USA) (Fig. 1). Present-day Bermuda is approximately 56 km^2; but the area was diminished significantly during maximum submergence of the last interglaciation. During extreme interglacial highstands, such as that during MIS 11 (Hearty et al., 1999), subaerial Bermuda may have been reduced to a few rocky islets, periodically submerged and washed over by waves (Olson and Hearty, 2003).

In contrast to interglaciations, during glacial maxima, sea level fell over 100 m (MIS 4-2), at which time the Bermuda platform formed an extensive limestone plateau covering an area of up to 1000 km^2. Such major sea-level fluctuations modulate and drastically alter environmental conditions on the island. These spatial and ecological changes appear to govern the direction and tempo of evolution of the island's biota, elements of which must either adapt or perish.

1.1. Stratigraphic framework of Bermuda

The present land area of Bermuda consists almost exclusively of bioclastic carbonate deposits of Quaternary age (Land et al., 1967; Vacher et al., 1995). Only a minor percentage of volcanic and aerosol sediments infuse the nearly pure carbonate deposits. Even early observations (Sayles, 1931; Bretz, 1960) concluded that the surficial geology of the island is disproportionally represented by the eolianite deposits. Bretz (1960) and Land et al. (1967) established that eolianites originated during interglacial highstands, when the source shorelines were nearby. Interglacial eolianites thus comprise most of the formations and the vast majority of the island's volume, with minor percentages of marine facies nearer sea level. The early Pleistocene Walsingham Formation is the basal foundation of the surficial geology, which is overlain by the Lower and Upper Town Hill Formations of middle Pleistocene age (Vacher et al., 1989; Hearty et al., 1992; Hearty and Vacher, 1994). These are in turn, succeeded by the Belmont (since renamed), Rocky Bay, and Southampton Formations. These three formations are now (Hearty, 2002) associated with the last interglaciation (*sensu lato*, Table 1). Unlike the Bahamas (Hearty and Kaufman, 2001), there has been no significant eolianite buildup of sediments over Bermuda during the last several thousand years of the Holocene. Each formation is laterally interbedded with weakly consolidated horizons that are interpreted as weak soils, entisols (US Soil Survey, 1975), or protosols (Vacher and Hearty, 1989) that formed over hundreds or few thousand years as vegetation flourished on stabilized beach or dune surfaces. Fossils of interglacial age, mainly land snails, are most abundant in these interglacial intercalations.

Each interglacial limestone is locally capped by a *terra rossa* paleosol. Associated with glacial lowstands of sea level are red to reddish brown (5YR to 2.5YR ~4/6, Munsell, 1994) paleosols capping the limestones. These weathering deposits contain pedogenic horizons and are thus true soils. They are formed by the addition and weathering of atmospheric dust of probable Saharan origin (Glaccum and Prospero, 1980), which may contain a significant percentage (~20–60%) of insoluble grains typically consisting of illite, quartz, kaolinite, chlorite, and feldspar (Bricker and Mackenzie, 1970; Muhs et al., 1990; Foos, 1991). A fair amount of carbonate (generally over 50%) is contained in younger soil deposits.

Over the past two decades, extensive field work combined with multi-faceted geochronology programs by Hearty, Vacher, Olson and others have resulted in a much longer and more fully documented record of surficial deposits (e.g., Vacher et al., 1989; Hearty et al., 1992; Vacher et al., 1995) than perceived by either Land et al. (1967) or Gould (1969). Correlation of the interglacial deposits with odd-numbered isotope stages was established through various dating methods including uranium-series (Harmon et al., 1978, 1983; Ludwig et al., 1996; Muhs et al., 2002) and amino acid

Table 1
Correlation table of nomenclature associated with the stratigraphy of Bermuda

Land et al. (1967)	Vacher et al. (1989); Hearty et al. (1992)	Hearty (2002)	This paper, Cave and fissure stratigraphy	Correlated marine oxygen isotope stage (MIS)
Recent St. Georges Soil?	Recent St. Georges Soil?	Recent St. Georges Soil	Unit y/z and Grand Canyon Cave; Tom Moore's Cave	1
			Unit w/x	2/1
			Unit v and Wilkinson Q Rail fissure	3
			Unit uv	4
Southampton Fm	Southampton Fm	Southampton Fm	Unit u Wilkinson Q High fissure	5a
Spencer's Point		Pembroke dune (New name: Hungry Bay Fm)		5c
		Harrington Mb soil		5e/5c
Pembroke Fm Harrington soil Devonshire Fm	Pembroke dune Harrington soil Devonshire marine and dune	Devonshire Mb marine (max. +6–9 m), including Spencer's Pt. Rocky Bay Formation	Unit s/t	Late 5e
		Mid-5e regression; red colluvium	Unit r/s	Middle 5e
		Belmont marine (+2.5 m) (New name: Grape Bay Mb of Rocky Bay Formation)	Unit p/q/r	Early 5e
Shore Hills Soil	Shore Hills Geosol	Red geosol (?)	Unit o/∼p And Crane Fissure	Late 6 to early 5e
Belmont Fm	Belmont marine and dune (+2.5 m)	Harvey Rd Q. eolianite		7
	Ord Rd. Geosol	Ord Rd. Geosol		8
	U. Town Hill	Upper Town Hill		9
	L. Town Hill	Lower Town Hill +20 m highstand		11
	Unnamed?			12–26? BRS
?	Big Red soil (BRS)	Castle Harbour Geosol		
Walsingham Fm	Walsingham Fm	Walsingham Fm		27/35?

Units in Admiral's Cave and Wilkinson Quarry are correlated with marine isotope stages.

epimerization (AAE) techniques (Hearty et al., 1992; Hearty and Vacher, 1994; Hearty, 2002). The number of paleosol-bounded limestone units described, and the time represented by them has doubled or tripled since Gould (1969) attempted to reconstruct the biostratigraphy of the island's land snail fauna. Six to nine interglacial highstand cycles are probably represented (Table 1). This more complete time and rock stratigraphy of Bermuda, encompassing perhaps over one million years (Hearty and Vacher, 1994), offers the possibility of closer examination of the relationship between sea-level changes and evolutionary events. Recent discovery in caves and fissures of a previously missing part of the stratigraphic succession provides new data relating to environmental conditions on the island during glacial lowstands.

For simplicity of communication, we follow the systematics of Gould (1969) for *Poecilozonites*: viz: (1) *P. bermudensis* (subspecies *P. b. zonatus* and *P. b. bermudensis*), a smaller helicoid shell averaging approximately 20 mm wide and 8–9 mm high; and (2) *P. nelsoni* a large, low to very high spired, and robust shell averaging 30–35 mm wide and 12–32 mm high. A generally higher spire and rounded outside whorl edge distinguishes subspecies *P. b. zonatus* from *P. b. bermudensis*. Width/height ratios are: *P. bermudensis* = 2.3 and *P. nelsoni* = 2.7–1.0. Thus, except for juveniles, the *P. bermudensis* and *P. nelsoni* forms are easily distinguished on the basis of size characteristics. All values were determined from published types or vouchers (described in Gould, 1969) at the Museum of Comparative Zoology, Harvard University by PJH/SLO. Although we utilize Gould's (1969) systematics and associated morphologies, we are not committed to their status as species and subspecies.

2. Geologic setting and stratigraphy of the pitfall deposits

2.1. Admiral's Cave (ADC)

ADC is formed in largely recrystallized limestone eolianites of the Walsingham Formation (Table 1). Galleries extend several hundred meters underground (Fig. 2). One of these contains one of the largest pitfall talus accumulations known on the island. This conical debris accumulation formed against the gallery wall after the roof collapsed and the cavern opened to the surface sometime before 130,000 years ago (Fig. 3). The gallery is approximately 30 m high, and 40–50 m across, while the talus cone itself is approximately 12 m high, and 20 m across the base. Only a small fraction of the volume of the talus cone has been sampled.

In October 2000, a 1-m-wide pit was excavated about 3 m above the base of the talus cone in ADC. After 2 m of downward excavation, progress was halted by a massive flowstone of unknown thickness. The stratigraphic succession of fossils, flowstone, and sediments was logged and sampled using a 3-dimensional coordinate system. Sample locations were further documented with x and y coordinates relative to surveyed horizontal and vertical baselines. Abundant fossils are present in the talus, and were similarly logged by layer and coordinates.

Twelve distinct flowstone, sediment, and fossil layers (inclined at about 25–30°) were labeled from oldest (level "o") to youngest (level "z"), along with several subunits ("z1", "z2", etc.). Fig. 4 illustrates the lithostratigraphic units and chronostratigraphy from the excavation at ADC. Three major, dense, clean, and creamy-white flowstone units were identified, along with at least five minor lenses that were generally mixed with soil debris giving them a "dirty" brown color. Thus flowstone varied from 100% pure calcite, to slightly less in the case of the sediment-tainted samples. Flowstone units "o" and "z" form the base and cap of the sequence, respectively, while a distinct ledge is formed from a dirty flowstone "w" in the upper layers. A stalagmite 40-cm-high is deposited on "t" and is buried by "v", and is thus referred to as the "tuv flowstone". Other localized, lenticular dirty flowstones occur in layers "s" and "uv".

Sediments were described and larger fossils removed by hand during the course of excavation. Bulk samples

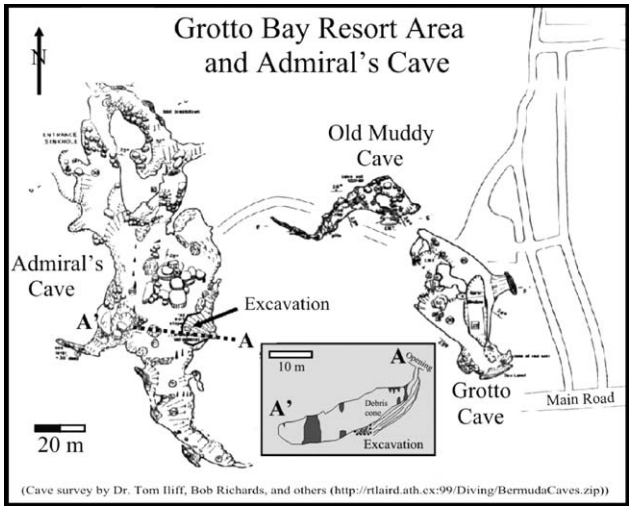

Fig. 2. Map of Admiral's and surrounding caves near and beneath Grotto Bay Resort. A cross-section of the debris cone is shown in the inset. The caves are developed in early Pleistocene eolianites of the Walsingham Formation.

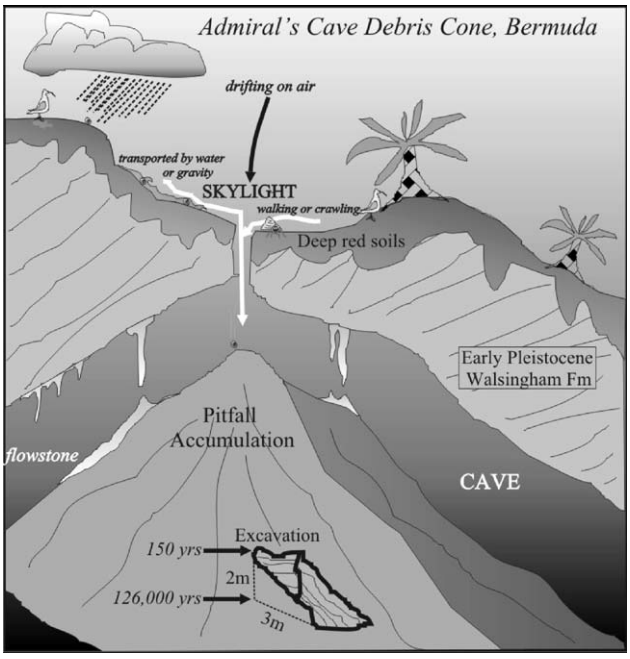

Fig. 3. Schematic illustration of the Admiral's cave skylight, pitfall accumulation, and excavation. At present, a small drainage catchment of approximately 200 m^2 drains directly into the cave.

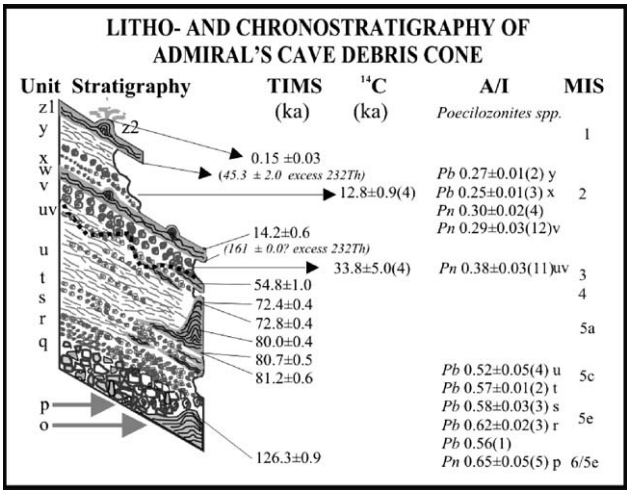

Fig. 4. Litho- and chronostratigraphy of the excavated pitfall deposits in the Admiral's Cave debris cone.

Table 2
Wet sediment colour (Munsell, 1994) and sedimentology of fissure and beds from Admiral's Cave

Field number	Wet color	% $CaCO_3$	Texture/composition
UWQ1d (rail fissure)	7.5YR 3.5/4	Trace	Silty clay
UWQ1d (reprep)	5YR 3.5-4/4	Trace	Silty clay
A(4/0) level y	7.5YR 4/6	86	Silty clay
A(4/0) level x	7.5YR 4/4	83	Silty clay
A(2 × 5.5) level v	10YR 5/4	90[a]	Fossils in silt
A(2.7 × 5.5) level uv	10YR 4/2	89	Fossils in clayey silt
A(2.5 × 6.7) level u	10YR 4/3	87	Clayey silts
A(2.2 × 6.5) level t	10YR 6/3	89	Sand/silt
A(2.5 × 6.7) level s	7.5YR 4.5 × 4	82	Sand/silt
A(2.5 × 6.7) level r	10YR 6/3	92	Sand/organics
A(2.4 × 5) level p	10YR 5.5/4	90	Fossil/silts
A(2.7 × 6.3) level p1	7.5YR 6/6	84	Clays

[a] Mostly composed of secondary cements and shell carbonate.

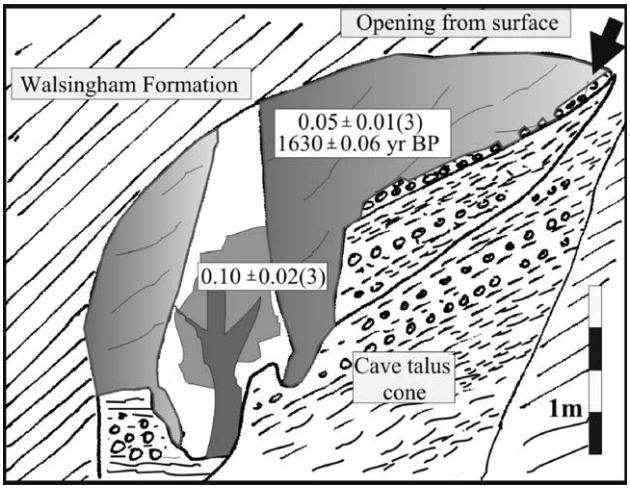

Fig. 5. Schematic drawing of the pitfall deposits in Grand Canyon Cave.

of approximately equivalent volume were collected from each level for graded sieving. Nine of the sedimentary units range from fine silt to coarse limestone cobbles, and contain variable concentrations of snail, crab, bat, and bird fossils. Some units, such as "r" and "t", are composed of nearly pure *Poecilozonites* shells with little sedimentary matrix, while others, such as "s" and "y", are mainly matrix with few fossils. Carbonate content for all non-flowstone units varies between 80% and 90% (Table 2), reflecting their relative youth among the carbonate landscapes on the island. Pedogenic stains are responsible for a very narrow spectrum of color (Munsell, 1994) among the cave deposits (Table 2). Charcoal is interspersed throughout the section with conspicuous concentrations in several levels. Unit "q" of coarse, brecciated, angular limestone cobbles, is apparently formed primarily of roof collapse material. This contains essentially no finer sediment from the levels above, the dense accumulation of nearly pure shells of *P. b. zonatus* capping it presumably having impeded the downward passage of silt. The thin, irregular patches of fine silt among the shells of *P. nelsoni* and other fossils in level "p" may represent the little sediment that could sift through from above that accumulated on the underlying flowstone (level "o").

2.2. Grand Canyon Cave (GCC)

GCC was explored and sampled in February 2001. The cave is of smaller and simpler geometry than ADC with enlargement of the cave along a fracture system adjacent to Castle Harbour. Materials from the outside are currently transported into the cave through a small, narrow sloping entrance, which appears to be an enlarged fissure zone. Sediment is also likely entering through obscured roof openings. A relatively small but active talus accumulation beneath one of the hidden skylights exposes numerous layers of shells, bones, and reddish brown sediments. The uppermost of these layers contains exotic land snail species (Beiler and Slapcinsky, 2000) with a fresh appearance and some human refuse, suggesting that it may have accumulated during the past few hundred years. Older deposits (Fig. 5) were collected from a 0.5-m-thick exposure near the base of the talus accumulation. These collections of sediment, charcoal, and land snails from GCC are younger than, and complete the succession from ADC.

2.3. Fissure deposits

Most of Bermuda's fissures occur in early and middle Pleistocene rocks, especially the Walsingham Formation, and are located in the eastern part of the island, particularly around Castle Harbour (Hartsock et al., 1995). This circular embayment may have been formed by the collapse of the ancient caldera of the volcanic seamount upon which the carbonate phase of Bermuda is built (Reynolds and Aumento, 1974). Fractures are oriented either perpendicular to, or circumferentially around Castle Harbour (Scheidegger, 1976; Hartsock et al., 1995). The bedrock walls of most fissures that we have observed are coated with cm-thick flowstone that appears to have filled the initial fracture.

Operations at Wilkinson and Government quarries have exposed (and consequently destroyed in most cases) numerous fossiliferous caves or fissures. The first of these to reach paleontological prominence was a cave exposed in Wilkinson Quarry about 1956 that contained bones of birds "with quantities of shells of land mollusks, [that] were imbedded in a calcareous tufa" (Wetmore 1960, p. 1). Extinct endemic birds in these deposits named by Wetmore (1960) were a crane (*Grus latipes*) and a duck (*Anas pachysceles*), plus two species of flightless rails (*Rallus ibycus, Porzana piercei*) that were named later by Olson and Wingate (2000). This

combination of species of birds is what is now referred to as the "crane fauna".

The next important fissure deposits were exposed in Government Quarry in 1960 and were collected by David Wingate with assistance from Pierce Brodkorb, Gould, and others. One of these, deemed "Crane Crevice" yielded the same "crane fauna" as described by Wetmore (1960) from Wilkinson Quarry. This is the locality that Gould (1969) called "Bird Fissure." Gould (1969) also mentions several other fissures in Government Quarry from which he obtained fossil snails, the most interesting perhaps being "Graveyard Fissure," which was dominated by the snail *P. b. zonatus*, which as we shall show is an indicator of the last interglacial period (MIS 5). Another opening collected by Wingate and Brodkorb, "Rail Cave," contained deposits lacking any of the species of the "crane fauna" and were dominated by bones of a much larger species of extinct, flightless rail, *Rallus recessus* (Olson and Wingate, 2001). The large snail *P. nelsoni* was found in both the "crane" and the "large rail" faunas. It became clear that these distinct avian faunas must represent different time periods, probably glacial episodes when land area was much greater, and it was speculated that the "crane fauna" was probably the older of the two (Olson and Wingate, 2001). Still, there were no absolute or relative dates for any of these fissure deposits.

Another productive site collected in 1999–2002 (PJH and SLO) was a vertical, sediment-filled fissure in Wilkinson Quarry (designated UWQ1d) that was exposed only a few hundred meters west of Admiral's Cave (Fig. 6). This fissure produced large amounts of shells of *P. nelsoni* and numerous bones of the large rail and other smaller birds. Another fissure (UWQ2f) collected for this study is located on the eastern flank of Wilkinson Quarry, but extended upward into the Lower Town Hill, overlying the Walsingham Formation. The fissures and their contents have no obvious internal structure or stratigraphic context, other than being younger than their host rocks, and their ages have long been a matter of speculation (Gould, 1969; Hartsock et al., 1995).

2.4. The "Shore Hills" soil

Gould (1969) correlated reddish sediments associated with most cave and fissure deposits with the so-called Shore Hills soil, which he described (p. 414) as a "well-developed red paleosol of island wide extent". In 1960s terms, the Shore Hills was developed on the "Belmont formation" (Table 1). These vague terms regarding the Shore Hills are further obscured by confusion over the meaning of "Belmont Fm" itself. In the context of recent definitions (Vacher et al., 1989; Vacher et al., 1995), Gould's Shore Hills could be nearly any red soil from last interglacial to early Pleistocene age

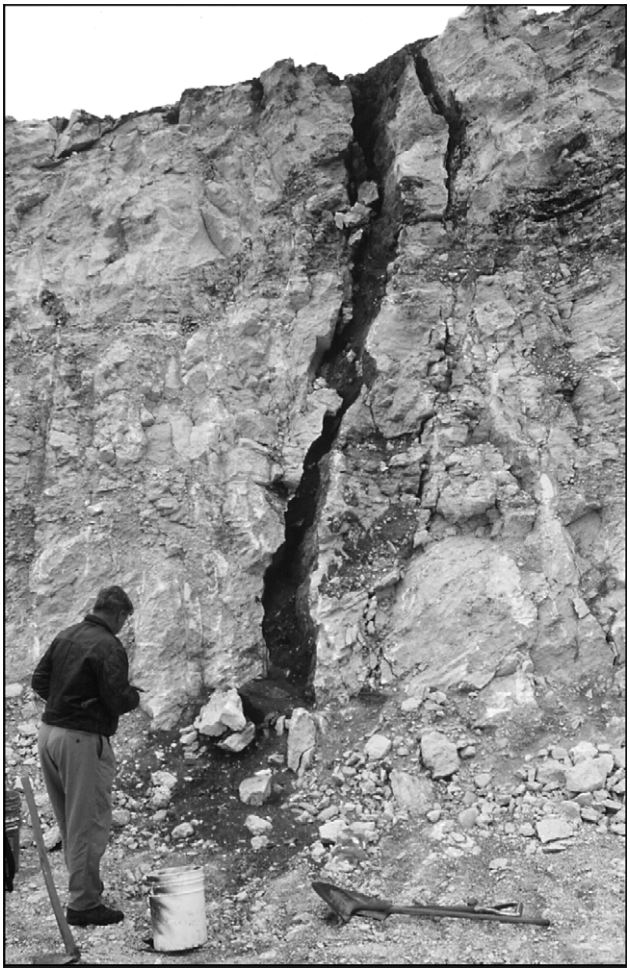

Fig. 6. The 1999 excavation of the "Rail Fissure" (UWQ4d) in Wilkinson Quarry. The site is located about 1 km west of Admiral's Cave. This fissure deposit, dated at 29,510±210 ^{14}C yr BP (Beta 165538), has produced abundant land gastropods and avian fossils (Olson and Wingate, 2001).

(i.e., 140,000 to >1 Ma). He also considered that the older Walsingham Formation was capped by an unnamed soil characterized as "a reddened surface rarely seen in the Walsingham district" (p. 414). In reality, by far the best-developed red paleosol in Bermuda, generally exposed in quarries, is what is now known as the Castle Harbor geosol that lies directly on the Walsingham Fm (Fig. 7). This soil may be up to 2 m thick and in Wilkinson Quarry may be seen penetrating several meters deep into the Walsingham limestone.

3. Geochronology

3.1. Amino acid epimerization (AAE) geochronology

AAE provides an independent measure of the relative age of land snail samples both inside caves and fissures and on the island's surface. The method is effective for

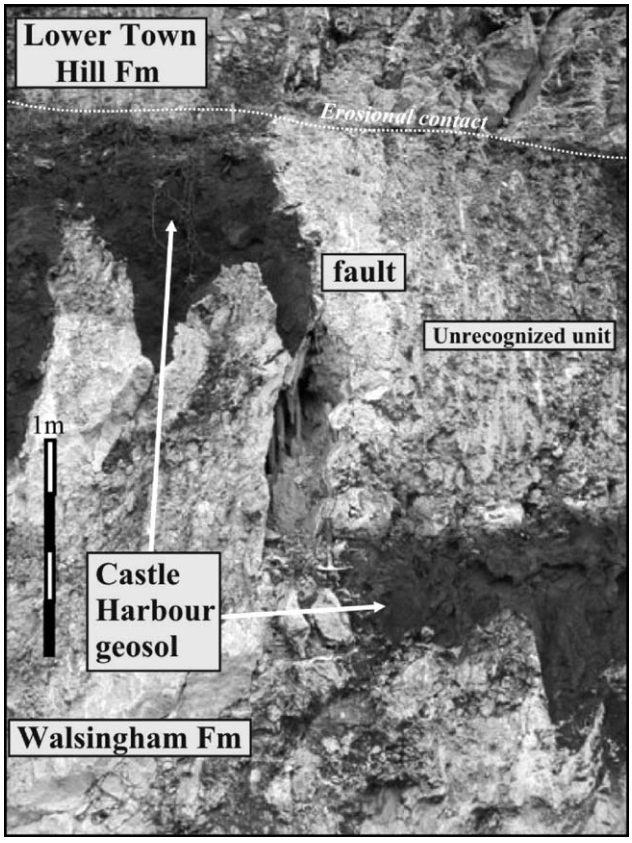

Fig. 7. Deep red soils and karstic surface associated with the Castle Harbour geosol (Vacher et al., 1989) (or "Big Red Soil" of Hearty and Vacher, 1994), which is developed on the Walsingham Formation. This paleosol and outcrop in Government Quarry is offset by approximately 1.5 m of faulting on a near-vertical plane.

over 1 Ma and has facilitated a greater understanding of the Quaternary stratigraphy of Bermuda (Hearty et al., 1992; Hearty, 2002). The background and procedures are detailed in Appendix A and references cited therein. *Poecilozonites* land snails occur in nine of the 12 units in ADC, in several units in GCC, and in all fissures examined. They are similarly abundant in surface exposures across the island (Gould, 1969; Hearty et al., 1992), but primarily in weak soils ("protosols") in eolianite.

The results from ADC and GCC, and several fissures are considered in the context of the existing AAE database for Bermuda for which 78 marine shells, nearly 104 *Poecilozonites* shells, and 83 whole-rock samples have been previously analyzed (Hearty et al., 1992; Hearty, 2002). Between 1992 and the present, considerably more marine shells, *Poecilozonites* shells, and whole-rock samples were analyzed. The combined *Poecilozonites* AAE dataset now comprises over 300 shell samples from deposits spanning a broad range of ages on the island except the Walsingham Formation, from which we have only two specimens of snail. This study focuses on results from cave and fissure deposits ($\sim$110 snail samples), but the results will be compared with the framework established by the full body of the available AAE database.

From ADC, the average *Poecilozonites* aIle/Ile ratios fall into correct stratigraphic order from the base to the top of the succession (Fig. 4; Table 3). Mean ratios for *P. nelsoni* and *P. bermudensis* range from 0.65 ± 0.05 (5) at the base of the ADC succession to 0.30 ± 0.02 (4) at level "x". AIle/Ile ratios are presented in the format 0.65 ± 0.05 (5), indicating the mean (0.65), $\pm$ one standard deviation or 1σ (0.05), and number of shells sampled in parentheses (5) comprising the mean.

Filling out the younger range of deposits from GCC and Tom Moore's Cave, *P. b. bermudensis* (Gould's "SJG" collection) yield considerably lower ratios (0.097 ± 0.023 (3); 0.072 ± 0.023 (3); 0.055 ± 0.034 (2) of SJG 53 (from Tom Moore's Cave): and 0.047 ± 0.014 (3) confirming other evidence for a younger age for these deposits. The aIle/Ile ratio for a then-living, now 100-yr-old *P. b. bermudensis* collected by Gulick (1904) is 0.017 ± 0.001(1).

3.2. Potential mixing in cave levels

Results from *Poecilozonites* demonstrate stratigraphic superposition in all cave levels, within standard error, and indicate that little mixing has occurred between levels. In four cases from ADC, however, one of the several aIle/Ile ratios (italicized in Appendix B) was far different from the others in its level. The anomaly could be considered a result of mixing, but in the majority of cases, the odd value was lower than the mean. The unexpectedly low ratios suggest that either the amino acid in these shells were leached or contaminated, or that younger shells were translocated to lower stratigraphic levels. No known large burrowing or digging organisms are known from Bermuda caves that are capable of significant bioturbation of sediment. Excluding these few ($\sim$4.5%) odd values from ADC reduces the variance about the mean, but does not change the age-ranking determined from the mean. In one case in GCC, a single *P. nelsoni* produced a significantly higher ratio (0.32) than several surrounding *P. bermudensis* (0.05 ± 0.01 (3)) from the same level (Appendix B). The higher ratio corresponds well with ratios from older levels in ADC containing exclusively *P. nelsoni*, thus indicating an isolated case of reworking of an older shell into younger deposits.

3.3. Whole-rock AAE

The chronostratigraphy of the surficial deposits of Bermuda was established in part on the basis of bioclastic limestone whole-rock samples (Hearty et al., 1992; Hearty, 2002). In those studies, aIle/Ile ratios established the temporal relationship between marine

Table 3
Isoleucine epimerization data from *Poecilozonites* spp. and whole-rock samples from the Admiral's and Grand Canyon Caves

Level, sample no., or Fm[a]	aIle/Ile[b] P. bermudensis	aIle/Ile[b] P. nelsoni	aIle/Ile[b] Whole-rock samples	Age ^{14}C yr BP	TIMS U/Th age (ka)	MIS Correlation
Z2	Flowstone	Flowstone		Flowstone	150±30 years	Modern
GC Cave UGC1z(2)	0.047±0.001(3)	0.323±0.008(1) *(reworked from x or older)*		1630±60		Late 1
Tom Moore's Cave (SJG53)	0.055±0.034(2)					Late 1
GC Cave UGC1z(1)	0.072±0.023(3)					Late 1
GC Cave UGC1x(2)	0.097±0.023(3)					Mid-1
z1					*(45.3±2)* Excess ^{232}Th	Mid-1
y	0.274±0.005(2)					
x	0.207±0.002(1) 0.253±0.011(3)	0.301±0.020(4) *(0.144; 0.209)*		12,800±50 12,960±50		2/1
w	Flowstone	Flowstone		Flowstone	14.2±0.6	
v		0.285±0.029(12) *(0.096)*				
uv		0.383±0.030(11) *(0.203)*		35,090±500 40,160±800		3/2
Lower uv		Intermittent	Flowstone		54.8±1 *(161.8±4)* Excess ^{232}Th	4
tuv		Intermittent	Flowstone		72 to 80	5a
u	0.524±0.054(6)	0.42(1) (Reworked)				5c
t	0.571±0.010(2) *(0.462)*		0.27(1)			Late 5e
s	0.582±0.034(3)		0.34(1)			
r	0.616±0.023(3)					
q						
p	0.564 (1)	0.650±0.065(5)				6/5e
o	Flowstone	Flowstone		Flowstone	126.3±0.9	6/5e

Values excluded from the mean are shown in parentheses and italics.
Wehmiller (1984) Standards 3/01 to 3/02: ILC-A = 0.146±0.006 (18); ILC-B = 0.473±0.013 (18); ILC-C = 1.016±0.020 (17).
[a] Admiral's cave levels (lower case alphabet) shown in Fig. 4; stratigraphic nomenclature in Table 1.
[b] Mean ratio, ±1σ of (n), the number of specimens analyzed.

and eolianite deposits. However, sieved carbonate sands in ADC of the 250–850 μm fraction were sufficiently abundant in only two samples to determine the aIle/Ile ratio of whole-rock. Units "s" and "t" produced whole-rock aIle/Ile ratios of 0.34 and 0.27, respectively, which correspond reasonably well with a peak MIS 5e mean aIle/Ile ratios for Belmont (0.40±0.02 (12)) and Rocky Bay Formations (0.32±0.02 (19)) for surficial whole-rock samples (Table 4), as well as with snails from those levels.

3.4. *Cittarium pica* results

The greater frequency of shell fragments of the rocky-coast dwelling top shell *C. pica* in levels "p", "q", and "r" in ADC, suggests the proximity of the coast to the cave skylight at the time of deposition of those levels. It is reasonable to assume that the *C. pica* shells accumulated at the shoreline and were subsequently transported overland to the cave by the hermit crab *Coenobita clypeatus* (Walker, 1994), remains of which also appear in ADC. Fragments of C. pica produce a mean of 0.70±0.06 (9), which overlaps at 1σ with the mean aIle/Ile ratio (0.76±0.05 (3)) from *C. pica* in the former Belmont Fm (Hearty et al., 1992), now assigned an early MIS 5e age (Hearty, 2002). The large intershell variation of aIle/Ile ratios from *C. pica* probably reflects their widely varied thermal and diagenetic history on land as they were used and traded among hermit crabs, perhaps over long periods of time.

Thus, by association with a nearby shoreline, and correlation of aIle/Ile results from both whole-rock and *C. pica* with surface deposits, we infer that cave levels "p", "q", "r", "s", and "t" were deposited during periods of high sea-level.

Table 4
Previously published and unpublished aIle/Ile data from the surficial geology of Bermuda (from Hearty et al., 1992and unpublished results)

Stratigraphic unit	AIle/Ile *P. bermudensis* and *P. cupula*	AIle/Ile Whole-rock	Estimated ~ or radiometric age	MIS correlation
Modern/Recent	0.017 (1)	0.12±01(2)	Living 1903	1
Southampton Fm	0.40±0.04 (36)	0.21±0.01(2)	82,000[a]	5a
Pembroke Mb		0.27±0.03(13)		
Harrington Mb-RBFm	0.49±0.03(36)		110,000	5c
Devonshire Mb-RBFm	0.59±0.03(19)	0.32±0.02(19)	120,000[a]	Late 5e
Former Belmont Fm Now Grape Bay Mb Rocky Bay Fm	0.61±0.05(10)	0.40±0.02(12)	128,000[a]	Early 5e
Harvey Rd Q.	—	0.49±0.04(11)		7?
U. Town Hill Fm	Pc	0.56±0.02(11)		9/11
	0.78±0.04(11)			
UWH2b	Pc			9/11
Albuoy's Pt.	0.82±0.04(3)			
Dead End Cave	Pc	0.69±0.01(6)	405,000±25,000[b]	11
L. Town Hill Fm	0.95±0.03(17)			
Walsingham Fm	—	1.11±0.02(3)	>780,000[c]	25–37

[a] Harmon et al. (1983); Ludwig et al. (1996); Muhs et al. (2002).
[b] Hearty et al. (1999); Hearty, Edwards, and others, unpublished.
[c] Hearty and Vacher (1994).

Table 5
Poecilozonites aIle/Ile ratios from fissure deposits in Bermuda. Refer to Gould (1969) for "SJG" locations

Fissure name	aIle/Ile *Poecilozonites bermudensis zonatus*	aIle/Ile *Poecilozonites nelsoni*	Approximate age	Proposed MIS correlation
Government Q.		0.161(1)	10–15,000	2/1
SJG5		0.328(1)		
"Main Fissure"				
Government Q.		0.305±0.014 (4)	12–15,000	2
UGQ81				
Baird Collection.				
Government Q.		0.316±0.003 (2)	12–15,000	2
Olson 1985		*(0.105)*		
UWQ1d		0.400±0.019 (8)	29,510±200	3/2
"Rail Fissure"		*(0.241)*	(Table 6)	
UWQ4		0.487±0.003 (2)	60–80,000	5a/4
Fissure collection from		0.735 (1)		
WQ—no info				
UWQ2f	0.499±0.009(3)		110,000–100,000	5d/5c
Fissure in LTH				
Government Q.	0.546±0.021(3)		125,000	5e
SJG5				
"Graveyard Fissure"				
UGQ68		0.623±0.018 (2)	140,000	6/5e
"Bird Fissure"				

Values excluded from the mean are shown in parentheses and italics.

3.5. aIle/Ile results from fissure deposits

The oldest fissure deposits in Government Quarry are from "Crane Crevice" (see Olson and Wingate, 2000, 2001). These deposits contain specimens of *P. nelsoni* with a mean aIle/Ile ratio of 0.62±0.02 (2), equivalent to an age ⩾126,000 years (Table 5). A *P. nelsoni*-bearing fissure in Wilkinson Quarry (UWQ1d) yielded a mean value of 0.40±0.02 (8) and an age of 29,510±200 ^{14}C yr BP. Collections of *P. nelsoni* from two other Wilkinson Quarry fissures, housed at the Smithsonian Institution (Baird's collection 1981, and Olson's 1985 collection), returned mean values of 0.31±0.01 (4) and 0.32±0.01 (2) (Table 5). These equivalent aIle/Ile ratios are associated with ages of circa 12,800 ^{14}C yr BP (Table 6). *Poecilozonites nelsoni* from Gould's (1969) "main fissure" in Government Quarry produced discordant values of 0.33 and 0.16. Two older Bermuda Museum collections from fissures in Wilkinson Quarry (UWQ4 and UWQ3) produced a mean of 0.48 with a single odd

Table 6
AMS Radiocarbon ages from Admiral's and Grand Canyon Caves, and the "Rail Fissure" (UWQ4)

Beta ID	Field ID	Sample material	$\delta^{13}C$ (‰)	Conventional radiocarbon age (yr BP)	Mean aIle/Ile (*P. nelsoni* or *P. bermudensis**)
Beta 165530	UGC1z(2)	Charcoal	−24.9	1630±60	0.05±0.01(3)*
OZG 458	A(4×0)x	Shell	—	12,500±80	0.21±0.002(1)+*
OZG 457	A(4×0)x	Charcoal	−25.0	12,870±80	0.21±0.002(1)+*
Beta 148571	A(4.0×0.0)x	Charcoal	−24.3	12,820±50	0.30±0.01(4)
Beta 165534	A(6.3×8.5)v	Shell	−9.5	10,280±50	0.28±0.03(3)
Beta 165535	A(2.7×5.5)v?	Charcoal	−24.1	12,750±50	0.27±0.03(3)
Beta 165532	A(2.7×5.5)uv	Charcoal	−24.5	12,800±50	0.28±0.04(2)+
Beta 165531	A(2.7×5.5)uv	Shell	−9.6	12,960±50	0.28±0.04(2)+
Beta 148570	A(2.5×5.8)v	Charcoal	−23.8	30,420±170	0.37±0.04(6)
Beta 165536	A(2.7×5.5)uv2	Charcoal	−24.1	35,090±500	0.40±0.01(2)
Beta 165533	A(2.7×5.8)uv	Charcoal	−25.3	40,160±800	0.41±0.05(2)
Beta 165538	UWQ1d	Shell	−9.6	29,510±210	0.40±0.03(3)

+Samples from same stratigraphic level and location (same bag).
Means: 33,800±5000 yr BP is equal to 0.40±0.03(7); 12,780±160 yr BP is equal to 0.28±0.02(12). AMS samples were determined at Beta Analytical ("Beta") and Australian Nuclear Science and Technology Organisation ("OZG").
*Species analysed is *P. bermudensis*.

value of 0.73, indicating that UWQ3 may be pre-MIS 5e age. Crane Crevice and UWQ1d fissures have produced distinctly different species of flightless rail (*Rallus ibycus and R. recessus*, Olson and Wingate, 2000, 2001).

Two fissures containing only *P. b. zonatus* in Government (Gould's, 1969 "Graveyard Fissure") and Wilkinson (Lower Town Hill fissure) Quarries produced mean values of 0.55±0.02 (3) and 0.50±0.01 (3) (Table 5). Both of these values place the time of fissure filling within the early half of MIS 5 (120,000–100,000 yr ago). With the exception of two unexpected results from Gould's "main fissure", the intershell variance in aIle/Ile from the fissure deposits is low, averaging ~3%. This low variance is similar to the natural variation among recent living and recently dead surface samples and reflect the rapid, episodic filling of fissures.

On the basis of aIle/Ile ratios, some fissure deposits are correlated with levels in ADC that contain the same morphotypes of *P. nelsoni* and *P. b. zonatus* (Table 5). ADC aIle/Ile ratios from levels "u" (0.50) and "t" (0.55) are equivalent to the Wilkinson Quarry (UWQ2f) and "Graveyard" fissures, all represented by *P. b. zonatus*. *P. b. zonatus* with mean ratios between 0.50 and 0.59 are typical the Harrington and Devonshire Members of the Rocky Bay Formation on the island's surface (Table 4).

3.6. Summary of aIle/Ile data

The aIle/Ile data from the succession of cave layers conform with stratigraphic order, and show little inter-unit mixing. The range of *Poecilozonites* aIle/Ile ratios, when compared to surface samples (Table 5), indicates estimated ages from early in the last interglaciation to historical times. The forms *P. b. zonatus* and *P. b. bermudensis* are well known and common in outcrops of last interglacial and Holocene sediment, respectively, and correlate with these ages on the basis of aIle/Ile ratios. The greater abundance of *C. pica* fragments and relative increase in coarse carbonate sand in the cave layers appears to correlate with a highstand event.

P. bermudensis yield ratios between 0.05 and 0.27 (generally *P. b. bermudensis*), and 0.52–0.62 (generally *P. b. zonatus*) (Table 3). Thus, the concordance of these observations allow a correlation of cave levels "r", "s", "t", and "u" with interglacial highstand conditions, probably the duration of MIS 5, while ADC level "x" and all GCC levels correlate with the initiation and duration of the current interglacial, the Holocene, MIS 1.

P. nelsoni, on the other hand, occurs only during the intervening glacial periods. Peak abundances of *P. nelsoni* have aIle/Ile ratios >0.62 and between 0.42 and 0.25. These intervals correlate with the penultimate glacial episode (up to the MIS 6/5e transition) and with the last (MIS 4-2) glacial period, respectively. Samples were analyzed from three transitional levels where both *P. bermudensis* and *P. nelsoni* were present. The two forms apparently epimerize at different but consistent rates. In examples from levels "x", "uv", and "p", the difference in the epimerization rate averages 20%, resulting in a mean *P. bermudensis*/*P. nelsoni* ratio of 0.80±0.06 (3). This quotient can be used to standardize between these two taxa in other levels.

3.7. AMS ^{14}C dating

Twelve accelerator mass spectrometry (AMS) ^{14}C ages were determined on both *Poecilozonites* land snails and charcoal from cave and fissure deposits (Table 6). An older group of ^{14}C ages of 30,420±200, 35,090±500, and 40,160±800 ^{14}C yr BP (Beta 148570, 165536, and 165533) on charcoal equate with an overall

aIle/Ile ratio on *P. nelsoni* of 0.40±0.03 (7), primarily from level "uv". A single *P. nelsoni* shell from fissure UWQ1d was dated at 29,510±210 ^{14}C yr BP (Beta 165538), and corresponds to a mean aIle/Ile of 0.40±0.02 (8) from *P. nelsoni* from the same fissure, and demonstrates that the fissure filled at the same time that sediment was deposited in level "uv" in ADC. The next younger cluster of ^{14}C ages of 12,820±50, 12,750±50, and 12,960±50, and 12,800±50 ^{14}C yr BP (Beta 148571, 165535, 165531, and 165532) (the latter two ages are from shell and charcoal from the same level) are associated with *P. nelsoni* with an overall mean aIle/Ile ratio of 0.28±0.02 (12) primarily from levels "v" and "x". Two additional samples of *P. b. bermudensis* (aIle/Ile = 0.21) and charcoal from level "x", produced AMS ^{14}C ages (OZG 458/457) of respectively, 12,500 and 12,850 ^{14}C yr BP. Six AMS ages from ADC converge on a mean of 12,780±160 ^{14}C yr BP, which corresponds within a hundred years of the initiation of the Younger Dryas (Broecker et al., 1988). Apparently this dramatic cooling of the North Atlantic Ocean not only had a major impact on surficial processes, but also on the viability of the island faunas of Bermuda, however, the specific causes and mechanisms are not clearly understood.

Among the youngest samples, charcoal from the upper unit "z" in GCC produced a calibrated age of 1630±60 ^{14}C yr BP (Beta 165530), corresponding to a *P. b. bermudensis* mean of 0.05±0.01 (3). The concordance between, and incremental increase among several ^{14}C ages and aIle/Ile ratios imply that the older ^{14}C ages are probably finite; thus acceptably accurate.

3.8. TIMS uranium-series dating

In situ and oriented flowstone samples collected from eight levels in the sequence were sliced with a rock saw into 60–100 g cubes. Sub-samples of hundreds of milligrams were drilled from these samples and analyzed at the University of Minnesota using TIMS uranium-series methods (see Appendix C). TIMS U-series analyses were determined on flowstone levels, "o", "tuv", "w" and "z:" which yielded ages ranging from 126,300±900 yr to 150±30 yr ago (Table 7). The results demonstrate stratigraphic order that largely agree with AAR and ^{14}C data in reasonable increments through the succession of twelve units, except in two samples, both of which had unusually high ^{232}Th contents, indicative of high detrital clay content and potentially high initial ^{230}Th.

The fact that both anomalous samples yield anomalously high ages (45,300±2000 and 161,800±400 yr BP; Table 7) out of stratigraphic order, supports the idea that the source of the discrepancy is high initial ^{230}Th. In principle, one can correct for initial ^{230}Th if one knows the initial ^{230}Th/^{232}Th ratio in each sample. However, high ^{232}Th samples, such as the two anomalous samples are very sensitive to initial ^{230}Th/^{232}Th value and therefore their ages cannot be corrected with accuracy and precision. Since we do not have independent knowledge of the initial ^{230}Th/^{232}Th of each sample, we have applied a generic correction using an initial ^{230}Th/^{232}Th value of 4.4±2.2 ppm (Table 7). The exact value of initial ^{230}Th/^{232}Th is not important for the 9 analyses of samples with relatively low ^{232}Th, as ages of low ^{232}Th materials are not sensitive to ^{230}Th/^{232}Th.

Table 7
Thermal ionization mass spectrometric (TIMS) ages from flowstone in Admiral's Cave debris cone

Sample number	^{238}U (ppb)	^{232}Th (ppt)	d^{234}U* (measured)	^{230Th}/^{238}U (activity)	^{230}Th Age (Ka) (uncorrected)	^{230}Th Age (Ka) (corrected)	d^{234}U$^{**}_{Initial}$ (corrected)
A(4.5×12.5)z2	92.5±0.3	70±10	89.1±7.7	0.00169±0.00019	170±30	***150±30***	89.1±7.7
A(4×0) z1	*133.5±0.0.1*	*18740±120*	*56.4±1.3*	*0.3845±0.0032*	*49,200±510*	***45,300±2000***	*64.1±1.5*
A(5×5)w	93.5±0.1	3723±45	43.5±1.6	0.1368±0.0016	15,340±190	***14,220±590***	45.3±1.6
A(2.7×5.8)uv (top)	99.5±0.2	6524±40	36.6±3.5	0.4208±0.0022	56,660±470	***54,820±1020***	42.7±4.1
A(2.7×5.8)uv (bottom)	*58.24±0.08*	*13300±130*	*57.6±3.1*	*0.8399±0.0052*	*168,000±2800*	***161,800±4000***	*91.0±5.0*
A(2.4×5)uv (I)	99.2±0.1	209±5	50.8±1.2	0.5120±0.0019	72,450±410	**72,400±410**	62.4±1.4
A(2.4×5)uv (II)	99.5±0.2	177±5	56.9±4.1	0.5173±0.0019	72,850±580	**72,800±580**	70.0±5.1
A(2.4×5)tu	239.3±0.3	439±5	47.2±2.0	0.5466±0.0014	80,020±390	**79,970±390**	59.2±2.5
A(2.4×5)st (A)	187.7±0.3	93±4	67.4±2.4	0.5615±0.0019	80,710±490	**80,690±490**	84.7±3.0
A(2.4×5)st (B)	119.1±0.1	170±6	60.4±1.2	0.5601±0.0027	81,280±590	**81,240±590**	76.0±1.6
A(2.2×5.9)o	129.7±0.1	27±4	27.8±1.7	0.7076±0.0023	126,310±880	**126,310±880**	39.7±2.4

Samples are presented in stratigraphic succession. All ages are in stratigraphic order except for samples "A(4×0)z1" and "A(2.7×5.8)uv (bottom)". We ignore the ages of these high-^{232}Th samples (italics) as they likely contain a large fraction of initial ^{230}Th, which is difficult to quantify (see text). $l_{230} = 9.1577 \times 10^{-6}\,yr^{-1}$, $l_{234} = 2.8263 \times 10^{-6}\,yr^{-1}$, $l_{238} = 1.55125 \times 10^{-10}\,yr^{-1}$.
*d^{234}U = ([^{234}U/^{238}U]$_{activity}$–1)×1000. **d^{234}U$_{initial}$ was calculated based on ^{230}Th age (T), i.e., d^{234}U$_{initial}$ = d^{234}U$_{measured}$ × el234 × T. Corrected ^{230}Th ages assume the initial ^{230}Th/^{232}Th atomic ratio of 4.4±2.2×10^{-6}. Those are the values for a material at secular equilibrium, with the crustal ^{232}Th/^{238}U value of 3.8. The errors are arbitrarily assumed to be 50%. A is younger than IB (~2 mm). I and II are the different fragments of the same sample.

Initial $^{230}Th/^{232}Th$ values lower than our generic value (Dorale et al., 1992) and much higher than our value (Beck et al., 2001) have been reported in speleothems. If we are allowed to choose $^{230}Th/^{232}Th$ values (within the broad range of reported values), we can find values that will correct the anomalous ages so that they are in the correct stratigraphic order relative to the other ages. However, as this choice is arbitrary, we choose instead to ignore the anomalous samples, and rely on the ages of the 9 samples with low ^{232}Th values.

The uppermost 2-cm of the level "o" flowstone produced the oldest ADC age of 126,300 ± 900 yr. As the sample was taken from the apex of a thick stalagmite, the age represents the cessation of flowstone accumulation for that speleothem. The thickness of the flowstone also suggests that deposition must have been initiated during MIS 6, and continued through Termination II (MIS 6/5e boundary), up to the beginning of MIS 5e. Fossils and sediments adjacent to level "o" may thus date from the same interval of MIS 6/5e transition, or indeed may be leftovers of the penultimate glacial period.

The "tuv" flowstone centers on MIS 5a/4 transition dated between 81,200 ± 600 and 72,600 ± 500 yr. This interval corresponds to the most rapid global buildup on ice, which took place between 76,000 and 71,000 yr (Cutler et al., 2003). Sample "uv" was split into stratigraphically lower ("uv1") and upper ("uv2") subsamples separated by 2 mm, and yielded sequential ages of 72,800 ± 600 and 72,400 ± 400 yr. This test demonstrates the integrity of the pure, milky flowstone material for TIMS dating. The next higher lenticular flowstone yielded an age of 54,800 ± 400 yr, while a thin, but extensively tainted sample from "w" returned an age of 14,200 ± 400 yr. The level "w" TIMS age is bracketed above and below by ^{14}C dates from levels "v" and "x" of circa 12,800 yr BP. The upper 2 cm of level "z" from an active flowstone at the top of the ADC succession returned an age of 150 ± 30 yr.

3.9. Epimerization kinetics from Poecilozonites land snails

When numeric ages and aIle/Ile ratios are combined and standardized to *P. bermudensis* ($aIle/Ile_{Pn} = 1.20 \times aIle/Ile_{Pb}$) a kinetic pathway for *Poecilozonites* can be constructed (Fig. 8). Results show a strong non-linearity in the natural epimerization rate, characterized by four distinct phases: (*Phase I*) an early phase of rapid epimerization during the initial (Holocene) phase of the reaction for samples that have only experienced warm, interglacial conditions; (*Phase II*) a slow intermediate phase in response to the cool conditions during the last glaciation; (*Phase III*) a second rapid phase during warm interglacial climate; and (*Phase IV*) beyond the last interglaciation, a rapidly decreasing rate into the slowest sub-linear phase of the epimerization reaction. The curve extends outward to the Lower Town Hill Fm, whose aIle/Ile values 0.95 ± 0.03 (17) is constrained and calibrated by TIMS flowstone ages of 405,000 ± 25,000 yr (Hearty et al., 1999; Edwards, Cheng, and Hearty, unpublished). The flowstone directly overlies intertidal and supratidal deposits containing fossil snails in a sea cave exposed in Government Quarry (Olson and Hearty, 2003).

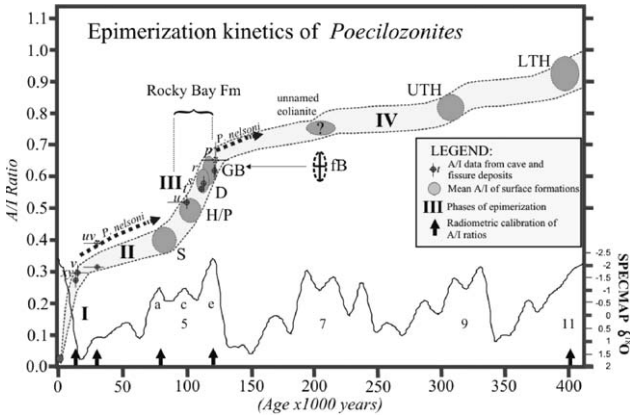

Fig. 8. Extent of epimerization (aIle/Ile) in fossil snails for Admiral's Cave and outcrops from the island surface. A SPECMAP $\delta^{18}O$ isotope curve (Imbrie et al., 1984) is provided for reference. Phases of epimerization are explained in the text. Abbreviations: LTH, Lower Town Hill Fm; UTH, Upper Town Hill Fm; fB, former Belmont Fm; GB, Grape Bay Mb; D, Devonshire Mb; and H/P, Harrington/Pembroke Mbs, all of the Rocky Bay Fm; S, Southampton Fm.

The significant rate changes in epimerization between Phases I and IV can be explained by the combined effects of the apparent parabolic kinetics of the reaction (APK, Mitterer and Kriausakul, 1989), and significant changes in natural temperature history in the region. Chapman and Shackleton (1998) calculated SST changes of 5–7°C between glacial and interglacial cycles in the North Atlantic at 40° North Latitude (8° north of Bermuda). Dramatic cooling events exceeding 10°C from interglacial conditions are centered at 65,000, 35,000, and 18,000 yr ago. These dramatic warming and cooling shifts in SST near Bermuda provide independent support of the reconstructed kinetic pathway in Fig. 8: Phase I occurred during a warm period of fast epimerization; Phase II, cold climatic during slowing epimerization; Phase III, warm climate during slowing epimerization, and Phase IV, cyclical climatic fluctuations combined with an ever slowing epimerization rate.

4. Discussion

The major implications of this study fall into three categories: (1) physical processes of sedimentation in caves and fissures; (2) the biological and ecological reaction of Bermuda's exiled faunas to dramatic spatial

changes brought about by changes in sea level up to 120 m; and (3) inferences of climatic conditions on the oceanic island during extensive periods between interglacial highstands.

4.1. The role of AAE and independent calibration by ^{14}C and TIMS to decipher the timing and correlation of events since Termination II

The combination of stratigraphic relations and three independent dating methods provides a framework to assess the timing and rates of geological processes. This data set indicates that the rate of deposition of sediments and fossils increased in the talus accumulation in ADC during the MIS 5e interglaciation after 126,300 ± 900 yr. This increased rate can be attributed to the proximity of the shoreline, which concentrated loose sediment, abundant organisms, and detrital organic material in the vicinity of the cave. Land snail shells in level "r" accumulated in thick lenses of greater volume than clastic sediments. The sediments showed a greater abundance of carbonate sand, along with a conspicuous increase in shallow-marine *Cittarium pica* shells, presumably transported to the cave skylight by the hermit crab *Coenobita clypeatus* (Walker, 1994). These features provide evidence that the shoreline was near the cave during MIS 5e. During the maximum sea-level rise of MIS 5e, the cave opening is estimated to have been only 100 m from Castle Harbour, and 400 m from the higher energy North Shore. Rates of sedimentation slowed progressively over the course of MIS 5, presumably as sea level withdrew.

The end of MIS 5 is marked by a substantial accumulation of the "tuv" flowstone TIMS dated at 72,400–81,200 yr. A prolonged period of slower sedimentation and relative inactivity followed MIS 5a until the end of MIS 2 at circa 12,780 ± 160 yr BP. The slowed sedimentation may have been the result of a greatly enlarged island during glacial lowstands, dispersing faunal elements relative to the cave skylight. The Holocene is marked by a low sedimentation rate in ADC, in contrast to GCC, where significant deposition occurred in the cave. The most significant flowstone deposits coincide with climatic transitions between oxygen isotope stages at MIS 6/5e (Termination II), 5a/4, and 2/1 (Termination I).

4.2. Similarity of thermal histories in subterranean and subaerial deposits

When calibrated to numeric ages, our results indicate no discernable difference in the thermal histories of the cave deposits, when compared with deeply buried (> 1–2 m) samples on the island surface. This correlation is most elegantly demonstrated by the equality of surface and ADC levels "s" and "t" aIle/Ile ratios in *P. b. zonatus* of 0.59 ± 0.03 (19) and 0.58 ± 0.03 (5), respectively, during a peak highstand. AIle/Ile ratios in *P. b. zonatus* in levels "r", "s", "t" and "u", constrained between TIMS flowstone ages of 126,300 and 72,600 yr, are nearly identical to those from surficial deposits constrained by coral ages 130,000 and 80,000 yr (Harmon et al., 1983; Ludwig et al., 1996; Muhs et al., 2002). On the basis of our data, we conclude that levels "r", "s", and "t" are correlated with the former Belmont (now Grape Bay Member, Hearty, 2002) and Rocky Bay Formations (Table 1). These units were deposited during a period of interglacial highstands and oscillating sea levels of MIS 5e (Hearty and Neumann, 2001; Hearty, 2002).

Poecilozonites bermudensis zonatus from level "u" correlates with the Harrington soil (Hearty, 2002) on the basis of aIle/Ile ratios in land snails. For reasons that are not clear, there are no Southampton-equivalent *P. b. zonatus* aIle/Ile ratios (circa 0.40 ± 0.04) from the cave. During this time, however, there is a significant buildup of very pure flowstone. Shells of this age may have been scarce on the surface, or not sampled in the cave. Alternatively, for a period of time between *P. b. zonatus* aIle/Ile ratios of 0.35 and 0.48, the skylight to the talus cones may have been partially or fully blocked or covered by vegetation and/or sediment. One of the benefits of the AAE method is the ability to detect significant breaks in the deposition such as in this case.

Deposition resumed sometime before the emplacement of "uv" (< 54,800 ± 1,000 yr). From then until the early Holocene, only *P. nelsoni* accumulated in the cave, after which this form was supplanted by *P. b. bermudensis*.

Further resolving the long-standing question of the age of the south shore Belmont Fm, the results from ADC confirm that aIle/Ile ratios in *Poecilozonites* on the surface and in the cave (of < 0.62) are equal to or younger than the MIS 6/5e transition. Furthermore, typical "Belmont" aIle/Ile ratios from whole-rock and *C. pica*, equivalent between surface and cave deposits, are all equal to or younger than 126,300 yr. These data further verify the assertion that the Belmont Formation as defined by Vacher et al. (1989, 1995) was deposited in early MIS 5e (Hearty, 2002).

4.3. Timing and mechanisms of fissure formation

Gould (1969, p. 461) believed that "fissures were filled at different times within the Shore Hills soil, and each of several fissures within a locality may contain a distinctive fossil sample." His observation that each fissure contains fill with distinctive fossil content, form, and timing is correct, but the inference that all fissures are formed within the Shore Hills (sensu Bretz, 1960) is contradicted by our findings. Fissures have mean aIle/Ile ratios (Table 5) on *Poecilozonites* morphotypes

(in parentheses) of 0.62 (Pn), 0.55 (Pbz), 0.50 (Pbz), 0.40 (Pn), 0.32 (Pn), and 0.31 (Pn). These ratios and morphotypes correspond precisely with results from ADC cave levels "p", "s", "u", "uv", "v", and "v", respectively. Means of 0.40 ± 0.03 (7) and 0.28 ± 0.02 (12) have equivalent ages of $33{,}800 \pm 5000$ and $12{,}800 \pm 90$ ^{14}C yr BP. The "Rail fissure" in Wilkinson Quarry produced an aIle/Ile mean of 0.40 ± 0.03 (3) and a corresponding age of $29{,}510 \pm 210$ ^{14}C yr BP on shell material of *P. nelsoni*. Harmon et al. (1978, 1983) provided then elusive, but now meaningful α-counting U-series ages of $58{,}000 \pm 5000$ and $101{,}000 \pm 18{,}000$ yr on a nondescript fissure-wall flowstone from Wilkinson Quarry. These flowstone ages probably mark the initial fracturing, which was then followed by soil and fossil filling during MIS 4–2. We are not certain, but Harmon's sample may have come from an extension of one of our younger glacial-age fissures such as UWQ1d.

The highest three means correlate with the MIS 6/5e transition (0.62 on *P. nelsoni*) and MIS 5e (0.55 and 0.50 on *P. b. zonatus*). Thus, the fissure-forming events span the interval between Termination II and Termination I with no apparent bias toward glacial or interglacial timing.

Our studies of fissures reveal that, upon fracturing, depending on climate and groundwater conditions, flowstone would fill the initial mm- to cm-scale fracture. As it opened widely, the fissure would fill rapidly by the collapse of the capping deep red "Shore Hills" soils, generally associated with the Walsingham and Town Hill Formations. Hapless surface fauna such as land snails, flightless birds, and crabs, combined with organic material and slopewash deposits, would completely fill the fissures over a relatively short time. However, the materials filling the fissures are diachronous: the ancient deep-red soils are associated with an older middle or early Pleistocene age, while the surface faunas were living or recently dead, and thus penecontemporaneous with the opening of the pitfall trap. Gould (1969) did not recognize this diachrony, and incorrectly surmised that the fissure faunas were considerably older than they actually are, primarily as a result of their circumstantial association with deep red soils.

There are obvious implications for the contents of fissures, but also for the process and the underlying causes of fracturing (Hartsock et al., 1995). Glacial ages associated with fissures support the view of Aby (1994) who suggested that lower sea level and the release of hydrostatic confining pressures was an underlying cause for the fracturing of the steep margins of the Bahamas. However, in contrast, fissures formed during the peak of interglaciations (MIS 5e) contradict Aby's, (1994) model, and thus a more complicated mechanism is apparently required. Deep-seated movements in the volcanic caldera may be dictated by loading and unloading of the depression (i.e., Castle Harbour) in synchrony with rising and falling seas. Fracturing and movement on faults observed in Government Quarry (Fig. 7) may also be tied to such a mechanism from Bermuda's underlying caldera.

4.4. Changing land snail morphology

Most of the dominant players in Gould's (1969) land snail phylogenetic scheme are contained in the pitfall deposits of Bermuda. Land snail morphology is marked by abrupt changes in the succession in ADC, particularly in transitional levels between glacial and interglacials. In level "p", at the base of the ADC section, adjacent to a flowstone dated at $126{,}300 \pm 900$ yr, is a lens of *P. nelsoni*, yielding a mean aIle/Ile ratio of 0.65 ± 0.05 (5). This particular morphotype is considered to be a "holdover" from the MIS 6 glacial lowstand. At the onset of the MIS 5e interglaciation, despite a shrinking island and probable concentration of land organisms into a vastly smaller space, *P. nelsoni* is replaced abruptly, immediately, and exclusively by *P. b. zonatus* in prolific numbers. *P. b. zonatus* dominates both the island surface and the cave deposits (levels "r" through "u") between 130,000 and perhaps 75,000 yr ago. The form of *P. b. bermudensis*, however, was dominant on St. Georges Island during much of that period (Gould, 1969). *P. nelsoni* has not been found among cave deposits during this "small-island" interval, implying that none were on the surface. Some time after the depostion of the "tuv" flowstone ($72{,}400 \pm 410$ yr) *P. nelsoni* reappears in levels "uv", "v", and "x" (between 58,000 and about 13,000 yr ago), while *P. b. zonatus* disappears entirely.

In level "x" of ADC, scarce but whole shells of *P. b. bermudensis* are found among a mix of *P. nelsoni* fragments. The *P. b. bermudensis* form again becomes conspicuous at the time of the Younger Dryas around 12,500 ^{14}C yr BP (OZG 458, Table 6) and through the Holocene. These significant changes in *Poecilozonites* must have been the result of pressure from environmental (island size changes, geographic limitations, changing food sources), climatic (dry or very wet; fires?), or ecological (predation; competition?) conditions. However, the entire genus is thought to now be extinct on Bermuda as a result of human perturbation (Beiler and Slapcinsky, 2000), including the introduction of non-native species such as pigs, rats, and predatory gastropods (e.g. *Euglandina*).

4.5. Inferences on climate changes in the North Atlantic since Termination II reflected in pitfall deposits on Bermuda

As sea level rose during the penultimate deglaciation, Bermuda's island faunas were concentrated into

progressively smaller areas. *P. nelsoni* appears to have been significantly impacted during this interval, causing a dramatic change of form at the onset of MIS 5e. For brief period at the end of MIS 5e, Bermuda was significantly smaller relative to the present as a result of sea levels from +6 to +9 m (Hearty, 2002). All surviving indigenous faunas were crowded into a smaller and smaller areas and islets. Presumably these highstand demographics are responsible for a high rate of deposition of shells in ADC.

Climate conditions around Bermuda were distinctly tropical maritime and forests of sable palm flourished on the island. As today, these latitudes were almost certainly influenced by warm tropical waters of the Gulf Stream. The interglacial island landscape was interspersed with interior fresh water lakes, salt ponds and marshes, and luxuriant vegetation that would have attracted and supported migratory birds. These warm and maritime conditions, similar to present, apparently persisted until the end of MIS 5a.

The onset of glaciation in northern latitudes may have been signaled in Bermuda by greater rainfall, which is marked in ADC by increased flowstone accumulation between 81,000 and 72,000 years ago. Sedimentation slowed significantly in the cave, and *P. b. zonatus* was replaced by *P. nelsoni* in deposits younger than 72,000 years. The slowing sedimentation in the cave may have been associated with more luxuriant vegetation associated with greater rainfall during that interval. Chapman and Shackleton (1998) document regional SSTs had become significantly colder during glaciation, which appears to correspond with a slowing epimerization rate between 70,000 and 12,000 years ago (Fig. 8). Shutdown of the Gulf Stream at the end of MIS 5e is likely (Broecker, 1997), while Cortijo et al. (1999) point to evidence of initial warming, followed by rapid cooling of the North Atlantic at the end of the last interglaciation.

With sea levels falling over 60 m from MIS 5a to MIS 4 and over 120 m during MIS 2 maxima, the groundwater table would also have fallen this distance. Surface water on the island must therefore have been reduced to ephemeral ponds and marshes, temporarily perched on palaeosol aquacludes. The middle of the 50×30 km platform during glacial periods was probably enough of an open savanna to have supported a population of cranes (we only know this for MIS 6). At various points through the rise and fall of sea level, this area would have experienced abundant rainfall, enough to support these ephemeral ponds and marshlands.

Winters were probably cold and stormy, dominated by clashing continental and oceanic air masses along the polar front. Summers were perhaps milder but also stormy, as conflicting air masses and solar heating on the large, >1000-km^2-island must have spawned frequent convectional thunderstorms. It is apparent from the abundance of charcoal in cave levels, particularly "v" and "x", that fires generally increased during the glacial, "large-island "phase. Preliminary identification of charcoal samples indicates that most, but not all, are from the Bermuda cedar, *Juniperus bermudiana* (Lee Newsome, pers. comm.), which is now nearly extinct on the island due primarily to the cedar scale blight in the 1940s.

Termination I is heralded by increased flowstone deposition (level "w") in ADC, and greater sedimentation in GCC, perhaps both tied to an increase in rainfall. Several ^{14}C ages converge ($12{,}780 \pm 160$ ^{14}C yr BP) on the Younger Dryas, but any causal relationships between cave sedimentation, faunal changes, and this cooling event require further study. Certainly the Younger Dryas profoundly impacted the land snail fauna, as *P. nelsoni* disappeared and was replaced by *P. b. bermudensis* at precisely that time. Conditions during the earlier Holocene were apparently much like that of today.

5. Conclusions

Pitfall debris cones in caves offer an "hourglass" style, relatively continuous sampling of changing surface sediments and faunas present on Bermuda over the past 130,000 yr. On the other hand, fissures preserve "snapshots" of the island's fauna. The clastic and organic materials of soil, carbonate sand, and charcoal, land snails, crustaceans, and bird fossils are periodically encased by flowstone deposition.

A broad range of geographical and ecological conditions were modulated by climate and sea-level changes. The greatest environmental impact was a spatial one, with the area of the island available for biotic development growing and shrinking by two orders of magnitude. During full-glacial times, the size of the island increased dramatically to become an "island plateau", where presumably, ephemeral lakes, open grasslands broken by scrubby forests dominated the landscape. Hydrological conditions on the island were dramatically altered by falling sea level, as the fresh water phreatic lens was displaced from the island's surface to deep within the pedestal. During full interglacial highstands, the island shrunk, and presumably took on a fully maritime aspect. Interglacial sedimentation rates were substantially greater than during glaciations in the vicinity of the caves.

AIle/Ile ratios, primarily on various morphologies of the land snail *Poecilozonites*, provide a means to unite and correlate deposits both above and below the surface. TIMS and ^{14}C ages calibrate the aIle/Ile ratios. From these results we have determined that deposition in ADC and GCC began during Termination II, and continued up to historic times. Cave and fissure deposits

are correlated with members of the Rocky Bay Formation on the surface.

Significant cyclical changes in the shell morphology of *Poecilozonites* occur in relatively continuous successions in ADC and GCC. We observe that two major "species" recognized by Gould (1969), *P. nelsoni* and *P. bermudensis*, are alternately dominant in glacial and interglacial stages, respectively, between MIS 6 and 5, and again between MIS 4/2 and 1.

Fissure formation around Castle Harbour occurred during both highstands or lowstands, and may be linked with general loading and unloading of the ancient volcanic caldera during sea-level oscillations. The sediment and fossils in fissures are diachronous, containing ancient soils mixed with much younger surface faunas.

In response to shifting atmospheric and pressure cells, and ocean currents, wind and rainfall conditions must have changed significantly. Major flowstone formation in ADC is associated primarily with stage transitions: MIS 6 to 5e, MIS 5a to 4, and MIS 2 to 1. This fact is apparently tied to wetter climatic conditions during these times, and by inference, dryer in the interim. The combination of colder temperatures, greater land area, increased wind, lower ground water table, and generally higher pressure associated with greater continental and polar cells, must have likewise contributed to more arid conditions. A larger oceanic island would have generated summer convectional lightning storms, increasing grass and forest fires under savanna-like conditions.

Pitfall deposits of sediment and fossil in Bermuda record changes in the physical, hydrological, and ecological conditions on the island during interglacial and glacial cycles, from 130,000 years ago to the present. These deposits provide insights into changing physical and biological processes on Bermuda, and are unique among isolated oceanic islands of the world.

Acknowledgements

Initial funding for cave excavation was provided by the Bermuda Aquarium, Museum, and Zoo (BAMZ, Museum Curator, Dr. Wolfgang Sterrer). The project was made possible by the overall cooperation and support of the Bermuda Government including Conservation Officers D. Wingate and J. Madeiros. The Bermuda Ministry of the Environment and the Smithsonian Institution generously provided funding for the bulk of AAE and ^{14}C analyses. We are grateful to Grotto Beach Hotel for logistical support and running electricity into the cave. Fred Collier facilitated our study of Gould's specimens, while K. Burns measured museum specimens during our visit to the Museum of Comparative Zoology at Harvard University. Two AMS ^{14}C ages were funded by the Australian Institute of Nuclear Science and Engineering (AINSE grant to PJH, Australia). TIMS uranium-series dating was supported by NSF 9809459 to RLE. Support for field and laboratory logistics, as well as collaborative visits to the Smithsonian Institution was provided by a Queensland-Smithsonian Fellowship in 2001 to PJH. For support of field work and dating of specimens we thank the Alexander Wetmore Endowment, the Radiocarbon Fund, and the Office of the Associate Director for Research and Collections (Ross Simons), all of the National Museum of Natural History, Smithsonian Institution. This is contribution number #64 of the Bermuda Biodiversity Project.

Appendix A. Background and preparation procedure for AAE

The underlying theory and various applications of the AAE method are summarized in Hare and Mitterer (1967) and Rutter and Blackwell (1995). The ratio of D/L (D-alloisoleucine/L-isoleucine, or aIle/Ile) amino acids measures the extent of racemization, or "epimerization" in the case of isoleucine. In living organisms, the aIle/Ile ratio is initially zero ($\sim$0.01 with laboratory preparation) and increases to an equilibrium aIle/Ile ratio of about 1.3. In addition to independent molecular factors, the rate of the isoleucine epimerization reaction depends on the ambient temperature within the geologic deposit. In this study, we evaluate the assumption that the ambient temperature in the cave has remained approximately the same as deeply buried samples from outcrops at the island surface. This evaluation is conducted by comparing aIle/Ile ratios from independently dated deposits both in the cave and on the surface.

AAE samples were analyzed by liquid chromatography at the Northern Arizona University Amino Acid Laboratory (Kaufman). Land snails of the genus *Poecilozonites* are one of the most conspicuous and abundant components of the cave and fissure deposits. Past AAE studies on Bermuda have shown this pulmonate gastropod to be a reliable sample material in relative-age determinations of the host deposits (Harmon et al., 1983; Hearty et al., 1992).

Preparation procedures and details of the methodology are offered in Hearty et al. (1992) and Hearty and Kaufman (2000). *Poecilozontes* and *C. pica* shells were mechanically cleaned and then sampled from the base of the columella where it joins the aperture. Sample analyses followed standard procedures prescribed in Miller and Brigham-Grette (1989). Whole-rock samples were obtained from the 250–850 μm sieve fraction of the cave sediments, and were then washed and leached as standard fossil samples. Approximately 100 mg of each sample was first leached in dilute HCl to remove 30% of the sample weight and reduce the possibility of

contamination by removing any remaining cements or other organic residues on shell or grain surfaces. Approximate 30-mg subsamples were dissolved in 7 M HCl containing 6.25 μM norleucine (a non-protein amino acid used as an internal standard). Samples were flushed with N_2, sealed in sterile vials, hydrolyzed at 110°C for 22 h, then evaporated under vacuum. After rehydration, samples were injected onto an ion-exchange high performance liquid chromatograph (HPLC) that employs post-column derivitization in OPA and fluorescence detection.

Each sample solution was analyzed two to four times and the results were averaged. The analytical precision of peak-height aIle/Ile ratios was typically <3%. To monitor analytical drift and facilitate comparison with other laboratories, the Amino Acid Geochronology Laboratory routinely measures the Interlaboratory Comparative Standards of Wehmiller (1984) (Footnote, Table 3). Nine levels in the pit yielded shells of *Poecilozonites*. For AAE studies, from 2 to 8 individuals were analyzed per level. AAE results are presented in Tables 3 and 4 and Appendix B.

Appendix B

A summary of aIle/Ile data from pitfall deposits is given in Table 8.

Table 8
Summary of aIle/Ile data from pitfall deposits

Level no.	Sample no.	AAL #	Species	aIle/Ile Poe	Mean	Stdev	*N* =	Age*	stdev
Modern	Gulick, 1904	4081A	Pbb	0.017	0.017	0.001	1	100	
"Z"	UGC1z(2a)	3847A	Pbb	0.05	0.047	0.014	3	1630	60
"Z"		3847B	Pbb	0.059					
"Z"		3847C	Pbb	0.031					
"Z"	UGC1z(1)	3858A	Pbb	0.058	0.072	0.023	3		
"Z"		3858B	Pbb	0.059					
"Z"		3858C	Pbb	0.099					
"Z"	UGC1x(2)	3845A	Pbb	0.079	0.097	0.023	3		
"Z"		3845B	Pbb	0.123					
"Z"		3845C	Pbb	0.089					
"Y"	A(4 × 0)y	3737A	Pb	0.27	0.274	0.005	2		
"Y"		3737B	Pb	0.278					
"Y"			**Pb**	***N* ⇒ 2**	**0.274**	**0.005**			
"X"	UAD 1 h	2683A	Pn	*0.209*					
"X"		2683B	Pn	0.278	0.305	0.035	2		
"X"		2683C	Pn	0.327					
"X"	A(4 × 0)x2	3375A	Pb	0.261	0.253	0.011	3	c12,820	50
"X"		3375B	Pb	0.241					
"X"		3375C	Pb	0.258					
			Pb	***N* ⇒ 3**	**0.253**	**0.011**			
"X"	A(4 × 0)x1	3374A	Pn	0.305	0.3	0.007	2	c12,820	50
"X"		3374B	Pn	0.295					
"X"		3374C	Pn	*0.144*					
			Pn	***N* ⇒ 4**	*0.301*	*0.02*			
(is "v")		3739C	Pb?	0.221	0.221	0	1		
(is "v")	UGC1z(2b)	3864A	Pn	0.323	0.323	0	1		
"V"	A(2.7 × 5.5)v?	3850A	Pn	0.24	0.27	0.031	3	c12,750	50
"V"		3850B	Pn	0.302					
"V"		3850C	Pn	0.268					
"V"	A(6.3 × 8.5)v	3851A	Pn	0.289	0.284	0.026	3	s10,280	50
"V"		3851B	Pn	0.307					
"V"		3851C	Pn	0.255					
(is "v")	A(2.7 × 5.5)uv	3739A	Pn	0.306	0.309	0.004	2		
(is "v")		3739B	Pn	0.311					
(is "v")	A(2.7 × 5.5)uv	3862A	Pn	0.253	0.283	0.042	2	s12,960	50
(is "v")	Bag 3	3862B	Pn	*0.096*				c12,800	50
(is "v")		3862C	Pn	0.312					
(is "v")	A(2.7 × 5.5)uv2	3859A	Pn	0.254	0.254	0	1		
			Pn	***N* ⇒ 12**	**0.285**	**0.029**			
			Pb	0.221	0.221	0			

Table 8 (*continued*)

Level no.	Sample no.	AAL #	Species	aIle/Ile Poe	Mean	Stdev	$N =$	Age*	stdev
(is "uv")	A(2 × 5.5)v	3376A	Pn	0.362	0.369	0.01	3		
(is "uv")		3376B	Pn	0.38					
(is "uv")		3376C	Pn	0.366					
"UV"	A(2.7 × 5.5/5.8)uv	3377A	Pn	0.402	0.364	0.054	2		
"UV"		3377B	Pn	0.326					
"UV"		3377C	Pn	*0.203*					
"UV"	A(2.7 × 5.8)uv	3738A	Pn	0.374	0.374	0.001	2		
"UV"		3738B	Pn	0.373					
"UV"		3738C	juv Pn?Pb?	0.297	0.297	0	1		
"UV"	A(2.7 × 5.8)uv	3861A	Pn	0.44	0.405	0.05	2	c40,160	800
"UV"	Bag 1	3861B	Pn	0.37					
"UV"	A(2.7 × 5.5)uv2	3859B	Pn	0.399	0.399	0	1	c35,090	500
(is "uv")	A(2.5 × 6.7)u	3740A	Pn	0.416			1	RW?	
			Pn	***N* ⇒ 11**	**0.383**	**0.03**			
			Juv? PnPb	0.297	0.297	0			
"U"	A(2.5 × 6.7)u	3740B	Pbz	0.54	0.495	0.039	3		
"U"		3740C	Pbz	0.475					
"U"		3740D	Pbz	0.471					
"U"									
"U"	A(2.5 × 6.7)u	3378A	Pbz	0.516	0.552	0.058	3		
"U"		3378B	Pbz	0.522					
"U"		3378C	Pbz	0.619					
"U"				**6 ⇒**	**0.524**	**0.054**			
"T"	A(2.2 × 6.5)t	3379A	Pbz	0.578	0.571	0.01	2		
"T"		3379B	Pbz	*0.462*					
"T"		3379C	Pbz	0.564					
"S"	A(2.5 × 6.7)s	3380A	Pbz	0.557	0.582	0.034	3		
"S"		3380B	Pbz	0.567					
"S"		3380C	Pbz	0.621					
"R"	A(2.5 × 6.7)r	3382A	Pbz	0.59	0.616	0.023	3		
"R"		3382B	Pbz	0.629					
"R"		3382C	Pbz	0.629					
"P"	A(2.4 × 5)p	3741C	Pbz	0.564	0.564	0	1		
"P"									
"P"	A(2.7 × 6.3)p1	3384A	Pn	0.617	0.686	0.062	3		
"P"		3384B	Pn	0.704					
"P"		3384C	Pn	0.736					
"P"									
"P"	A(2.4 × 5)p	3741A	Pn	0.589	0.597	0.011	2		
"P"		3741B	Pn	0.605					
"P"			**Pn**	***N* ⇒ 5**	**0.65**	**0.065**			
			Pbz	0.564	0.564	0			
FISSURES									
Wilk Q	UWQ1d	2682A	Pn	0.391	0.397	0.008	2		
Wilk Q		2682B	Pn	0.402					
Wilk Q		2682C	Pn	*0.241*					
Wilk Q	SOSI	3370A	Pn	0.396	0.405	0.022	3		
Wilk Q		3370B	Pn	0.39					
Wilk Q		3370C	Pn	0.43					
Wilk Q	UWQ1d	3372A	Pn	0.411	0.398	0.027	3	s29,510	210
Wilk Q		3372B	Pn	0.416					
Wilk Q		3372C	Pn	0.367					
				***N* ⇒ 8**	**0.4**	**0.019**			
Wilk Q	UWQ4	3840A	Pn	0.485	0.487	0.003	2		
Wilk Q		3840B	Pn	0.489					
Wilk Q									
Wilk Q	UWQ2f	3372A	Pbz	0.489	0.499	0.009	3		

Table 8 (*continued*)

Level no.	Sample no.	AAL #	Species	aIle/Ile Poe	Mean	Stdev	$N =$	Age*	stdev
Wilk Q		3372B	Pbz	0.506					
Wilk Q		3372C	Pbz	0.501					
Wilk Q									
Wilk Q	UWQ3	3857A	Pn?	*0.486*	?		2		
Wilk Q		3857B	Pn?	*0.735*	?				
Gov. Q	UGQ81	3865A	Pn	0.312	0.305	0.014	4		
Gov. Q	Baird, 1981	3865B	Pn	0.295					
Gov. Q		3865C	Pn	0.292					
Gov. Q		3865D	Pn	0.322					
Gov. Q	UGQE1	3860A	Pn	*0.105*					
Gov. Q	Olson 1985	3860B	Pn	0.318	0.316	0.003	2		
Gov. Q	R. ibicus	3860C	Pn	0.314					
Gov. Q	SJG5	3926A	Pn	0.238	0.3	0.09	2		
Gov. Q	Main Fissure	3926B	Pn	0.362					
Gov. Q	SJG5	3916A	Pbz	0.52	0.546	0.021	3		
Gov. Q	Graveyard Fiss	3916B	Pbz	0.566					
Gov. Q		3916C	Pbz	0.539					
Gov. Q	UGQ68	3866A	Pn	*0.368*					
Gov. Q		3866B	Pn	0.636	0.623	0.018	2		
Gov. Q		3866C	Pn	0.61			91		
CITTARIUM									
(is <"r")	A(2.5 × 5.5)q	3383C	Cp	0.595	0.595	0	1		
"R"	A(2.5 × 6.7)r	3381A	Cp	0.654	0.664	0.009	3		
"R"		3381B	Cp	0.666					
"R"		3381C	Cp	0.671					
				***N* ⇒ 3**	**0.664**	**0.009**			
"Q"	A(2.5 × 5.5)q	3383A	Cp	0.728	0.729	0.001	2		
"Q"		3383B	Cp	0.729					
"P"	A(2.4 × 5)p2	3385A	Cp	0.702	0.737	0.067	3		
"P"		3385B	Cp	0.694					
"P"		3385C		0.815					
				***N* ⇒ 5**	**0.734**	**0.048**			
RB Fm	Dev. Bay W	3964AB	Cp		0.51	0.02	3		
Bel Fm	Saucos Hill	3957AC	Cp		0.76	0.05	3		
WHOLE-ROCK									
	A(2.7 × 6.5)t	3393A	W-R	0.219	0.268	0.07	2		
		3393B	W-R	0.318					
	A(2.5 × 6.7)s	3394A	W-R	0.378	0.344	0.048	2		
		3394B	W-R	0.31					

Ratios excluded from means are indicated by italics. Mean ratios are highlighted in bold.

Appendix C. Preparation and analysis of flowstone samples for TIMS U/Th dating

At the University of Minnesota, several hundred milligrams of sample was drilled from each speleothem sub-sample, dissolved in a clean room, and spiked with a mixed ^{229}Th–^{233}U–^{236}U spike. Purified separates of uranium and thorium were then obtained by co-precipitation with Fe and ion exchange techniques. The separates were dried down, taken up in a small amount ($<1\pm$l) of dilute nitric acid, and loaded on zone-refined rhenium filaments. The thorium fraction was loaded with graphite and analyzed with the single filament technique, whereas the uranium fraction was dried down as uranium nitrate and analyzed using the double filament method. For both uranium and thorium ion beams were measured on a Finnigan MAT 262 RPQ mass spectrometer using a MassCom electron multiplier operated in ion counting mode and the retarding potential quadrupole. Analyses were performed in peak-jumping mode. The isotopic data were refined using standard isotope dilution equations. Ages were calculated using half-lives presented in Cheng et al. (2000). Our overall procedure is a modification of those first presented by Edwards et al. (1987), with modifications detailed in Cheng et al. (2000).

References

Aby, S.C., 1994. Relation of bank-margin fractures to sea-level change, Exuma Islands, Bahamas. Geology 22, 1063–1066.

Beck, J.W., Richards, D.A., Edwards, R.L., Smart, P.L., Donahue, D.J., Hererra-Osterheld, S., Burr, G.S., Calsoyas, L., Jull, A.J.T., Biddulph, D., 2001. Extremely large variations of atmospheric C-14 during the last glacial period. Science 292, 2453–2458.

Beiler, R., Slapcinsky, J., 2000. A case study for the development of an island fauna: recent terrestrial mollusks of Bermuda. Nemoria 44, 100pp.

Bretz, J.H., 1960. Bermuda: a partially drowned late mature Pleistocene karst. Geological Society of America Bulletin 71, 1729–1754.

Bricker, O.P., Mackenzie, F.T., 1970. Limestones and red soils of Bermuda, discussion. Geol. Soc. Am. Bull. 81, 2523–2524.

Broecker, W.S., 1997. Thermohaline circulation, the Achilles Heel of our climate system: will man-made CO_2 upset the current balance? Science 278, 1582–1588.

Broecker, W.S., Andree, M., Wolfli, W., Oeschger, H., Bonani, G., Kennett, J., Peteet, D., 1988. The chronology of the last deglaciation: implications to the cause of the Younger Dryas event. Paleoceanography 3, 1–19.

Chapman, M.R., Shackleton, N.J., 1998. Millennial-scale fluctuations in North Atlantic heat flux during the past 150,000 years. Earth and Planetary Science Letters 159, 57–70.

Cheng, H., Edwards, R.L., Hoff, J., Gallup, C.D., Richards, D.A., Asmerom, Y., 2000. The half-lives of uranium-234 and thorium-230. Chemical Geology 169, 17–33.

Cortijo, E., Lehman, S., Keigwin, L., Chapman, M., Paillard, D., Labeyrie, L., 1999. Changes in meridional temperature and salinity gradients in the North Atlantic Ocean (30°–72°N) during the last interglacial period. Paleoceanography 14 (1), 23–33.

Curran, H.A., White, B., 1995. Terrestrial and shallow marine geology of the Bahamas and Bermuda. Geological Society of America Special Paper 300, 344pp.

Cutler, K.B., Edwards, R.L., Taylor, F.W., Cheng, H., Adkins, J., Gallup, C.D., Cutler, P.M., Burr, G.S., Bloom, A.L., 2003. Rapid sea-level fall and deep-ocean temperature change since the last interglacial period. Earth and Planetary Science Letters 206, 253–271.

Dorale, J.A., Gonzalez, L.A., Reagan, M.K., Picket, D.A., Murrell, M.T., Baker, R.G., 1992. A high-resolution record of Holocene climate change in speleothem calcite from Cold Water Cave, Northeast Iowa. Science 258, 1626–1630.

Edwards, R.L., Chen, J.H., Wasserburg, G.J., 1987. U-238, U-234, Th-230, Th-232 systematics and the precise measurement of time over the past 500,000 years. Earth and Planetary Science Letters 81, 175–192.

Eldredge, N., Gould, S.J., 1972. Punctuated equilibria: an alternative to phyletic gradualism. In: Schopf, T.J.M. (Ed.), Models in Paleobiology. Freeman, Cooper and Co., San Francisco, USA, pp. 82–115.

Foos, A.M., 1991. Aluminous lateritic soils, Eleuthera, Bahamas: a modern analog to carbonate paleosols. Journal of Sedimentary Petrology 61 (3), 340–348.

Glaccum, R.A., Prospero, J.M., 1980. Saharan aerosols over the tropical North Atlantic—Mineralogy. Marine Geology 37, 295–321.

Gould, S.J., 1969. An evolutionary microcosm: Pleistocene and Recent history of the land snail *P. (Poecilozonites)* in Bermuda. Bulletin of the Museum of Comparative Zoology 138 (7), 407–531.

Gulick, A., 1904. The fossil land shells of Bermuda. Academy of Natural Sciences of Philadelphia 56, 406–425.

Hare, P.E., Mitterer, R.M., 1967. Non-protein amino acids in fossil shells. Carnegie Institute of Washington Yearbook 65, 236–364.

Harmon, R.S., Schwarcz, H.P., Ford, D.C., 1978. Late Pleistocene sea level history of Bermuda. Quaternary Research 9, 205–218.

Harmon, R.S., Mitterer, R.M., Kriausakul, N., Land, L.S., Schwarcz, H.P., Garrett, P., Larson, G.J., Vacher, H.L., Rowe, M., 1983. U-series and amino acid racemization geochronology of Bermuda: implications for eustatic sea-level fluctuation over the past 250,000 years. Paleogeography, Paleoclimatology, Paleoecology 44, 41–70.

Hartsock, J.K., Woodrow, D.L., McKinney, D.B., 1995. Fracture systems in northeastern Bermuda. Geological Society of America Special Paper 300, 325–334.

Hearty, P.J., 2002. A revision of the late Pleistocene stratigraphy of Bermuda. Sedimentary Geology 153 (1–2), 1–21.

Hearty, P.J., Kaufman, D.S., 2000. Whole-rock aminostratigraphy and Quaternary sea-level history of the Bahamas. Quaternary Research 54, 163–173.

Hearty, P.J., Neumann, A.C., 2001. Rapid sea-level and climate change at the close of the last interglaciation (MIS 5e): evidence from the Bahama Islands. Quaternary Science Reviews 20, 1881–1895.

Hearty, P.J., Vacher, H.L., 1994. Quaternary stratigraphy of Bermuda: a high-resolution pre-Sangamonian rock record. Quaternary Science Reviews 13, 685–697.

Hearty, P.J., Vacher, H.L., Mitterer, R.M., 1992. Aminostratigraphy and ages of Pleistocene limestones of Bermuda. Geological Society of America Bulletin 104, 471–480.

Hearty, P.J., Kindler, P., Cheng, H., Edwards, R.L., 1999. Evidence for a $+20$ m middle Pleistocene sea-level highstand (Bermuda and Bahamas) and partial collapse of Antarctic ice. Geology 27, 375–378.

Imbrie, J., Hays, J.D., Martinson, D.G., McIntyre, A., Mix, A.C., Morley, J.J., Pisias, N.G., Prell, W.L., Shackelton, N.J., 1984. The orbital theory of Pleistocene climate: support from a revised chronology of the marine $\delta^{18}O$ record. In: Berger, A.L., et al. (Ed.), Milankovitch and Climate, Part I. D. Reidel Publishing Company, Dordrecht, pp. 269–305.

Land, L.S., Mackenzie, F.T., Gould, S.J., 1967. The Pleistocene history of Bermuda. Geological Society of America Bulletin 78, 993–1006.

Ludwig, K.R., Muhs, D.R., Simmons, K.R., Halley, R.B., Shinn, E.A., 1996. Sea-level records at ~ 80 ka from tectonically stable platforms: Florida and Bermuda. Geology 24 (3), 211–214.

Miller, G.H., Brigham-Grette, J., 1989. Amino acid geochronology: resolution and precision in carbonate fossils. Quaternary International 1, 111–128.

Mitterer, R.M., Kriausakul, N., 1989. Calculation of amino acid racemization ages based on apparent parabolic kinetics. Quaternary Science Reviews 8, 353–357.

Muhs, D., Bush, C.A., Stewart, K.C., Rowland, T.R., Crittenden, R.C., 1990. Geochemical evidence of Saharan dust parent material for soils developed on Quaternary limestones of Caribbean and western Atlantic islands. Quaternary Research 33, 157–177.

Muhs, D., Simmons, K.R., Steinke, B., 2002. Timing and warmth of the Last Interglacial period: new U-series evidence from Hawaii and Bermuda and a new fossil compilation for North America. Quaternary Science Reviews 21, 1355–1383.

Munsell, 1994. Soil Color Charts, 1994 (revised edition). Macbeth Division of Kollmorgan Instruments Corporation, New Windsor, NY.

Olson, S.L., Hearty, P.J., 2003. Probable extirpation of a breeding colony of Short-tailed Albatross (*Phoebastria albatrus*) on Bermuda by Pleistocene sea-level rise. Proceedings of the National Academy of Sciences 100 (22), 12,825–12,829.

Olson, S.L., Wingate, D.B., 2000. Two new flightless rails (Aves: Rallidae) from the Middle Pleistocene "crane fauna" of Bermuda. Proceedings of the Biological Society of Washington 113 (2), 356–368.

Olson, S.L., Wingate, D.B., 2001. A new species of large flightless rail of the *Rallus longirostris/elegans* complex (Aves: Rallidae) from the

Late Pleistocene of Bermuda. Proceedings of the Biological Society of Washington 114 (2), 509–516.

Reynolds, P.R., Aumento, F.A., 1974. Deep Drill 1972: potassium–argon dating of the Bermuda drill core. Canadian Journal of Earth Sciences 11, 1269–1273.

Rutter, N.W., Blackwell, B. (Eds.), 1995. Dating methods for Quaternary deposits: Newfoundland, Geological Association of Canada, Geotext 2, 125–167.

Sayles, R.W., 1931. Bermuda during the Ice Age. American Academy of Arts and Sciences 66, 381–468.

Scheidegger, A.E., 1976. Joints on Bermuda. Rivista Italiana di Geofisica e Scienze Affini 3, 101–105.

US Soil Survey Staff, 1975. Soil taxonomy, a basic system of soil classification for making and interpreting soil surveys? US Department of Agriculture, Soil Conservation Service, Agriculture Handbook No. 436, 754pp.

Vacher, H.L., Hearty, P.J., 1989. History of stage-5 sea level in Bermuda: with new evidence of a rise to present sea level during substage 5a. Quaternary Science Reviews 8, 159–168.

Vacher, H.L., Rowe, M., Garrett, P., 1989. Geologic map of Bermuda. Oxford Cartographers, UK (1:25,000 scale).

Vacher, H.L., Hearty, P.J., Rowe, M.P., 1995. Stratigraphy of Bermuda: nomenclature, concepts, and status of multiple systems of classification. Geological Society of America Special Paper 300, 269–294.

Walker, S.E., 1994. Biological Remanie: gastropod fossils used by the living terrestrial hermit crab, *Coenobita clypeatus*, on Bermuda. Palaios 9, 403–412.

Wehmiller, J.F., 1984. Interlaboratory comparison of amino acid enantiomeric ratios in fossil Pleistocene mollusks. Quaternary Research 22, 109–120.

Wetmore, A., 1960. Pleistocene birds in Bermuda. Smithsonian Miscellaneous Collections 140 (2), 1–11 (3 plates).